Advances in Consumer Research
https://acr-journal.com/
Volume-2 | Issue-5 | Nov: 2025
Original Researcher Article

Numerical Analysis Of The Mhd Nanofluid Flow Over A Nonlinear Stretching Sheet With Brownian Motion And Chemical Reaction.

K.Santhosh Kumar[1], Dr. P.Mangathai[2]

[1,2]Department of Mathematics, Anurag University, Venkatapur, Hyderabad, Telangana State, 500088, India.

Corresponding author,

Email ID : mangathai123@gmail.com

ABSTRACT
This work examines the continuous magnetohydrodynamic boundary layer flow of a nanofluid across a stretching surface, considering the influences of Brownian motion, thermophoresis, and chemical reactions in the context of suction/injection. A similarity transformation is utilized to convert the controlling partial differential equations into a system of coupled nonlinear ordinary differential equations. The equations are numerically solved employing a fourth-order Runge-Kutta method alongside the shooting methodology. Particular emphasis is placed on examining the impact of the Brownian motion parameter (Nb) on the nanoparticle concentration profile. The findings indicate that augmenting Nb improves the diffusive transport of nanoparticles, thus thickening the concentration boundary layer. The method's accuracy and convergence are confirmed, and the resulting profiles are graphically analyzed for different values of Nb. These findings elucidate the dynamics of nanofluid transport under nonlinear rheological and electromagnetic influences..
Keywords: Nanofluid, Brownian motion, chemical reaction, magnetic field, Runge–Kutta method..

1. INTRODUCTION:

Nanofluids, which are colloidal suspensions of nanoparticles ranging from 1 to 100 nanometers in diameter inside base fluids, have garnered considerable scientific attention owing to their superior thermal and mass transport characteristics. Applications spanning energy systems to biomedical devices increasingly depend on the meticulous regulation of heat and mass transmission in nanofluidic settings. Among the diverse categories of nanofluids, non-Newtonian formulations, such as the nanofluid, demonstrate shear-thinning behavior, rendering them more precise approximations of numerous real-world fluids encountered in industrial processes. A multitude of researchers have examined the behavior of diverse nanofluids and models, including Carreau fluid [1], Williamson fluid [2], Casson fluid [3], Sisko fluid [4], pseudoplastic fluid [5], and the Cattaneo-Christov[6] model.

Magnetohydrodynamics (MHD) pertains to the examination of the flow characteristics of electrically conductive fluids under the influence of a magnetic field. It elucidates the behavior of materials such as plasmas, molten metals, and ionic solutions when exposed to magnetic forces. MHD [7] is essential for magnetic confinement in fusion reactors, metallurgical processing methods, space propulsion systems, and solar and astronomical events. The interaction of a magnetic field with a conducting fluid produces a Lorentz force that counteracts the fluid's motion, functioning as a resistive force. This effect results in significant changes in flow dynamics, including variations in the velocity field and adjustments to thermal and solutal transport properties. "The dampening effects of the magnetic field influence flow stability, boundary layer thickness, and the rates of heat and mass transfer. Numerous scholars have progressively expanded classical boundary layer theory to incorporate the influence of magnetic fields, facilitating the analysis of increasingly realistic physical systems. Makinde (2005) [8] examined the influence of thermal radiation and chemical processes on magnetohydrodynamic boundary layer flow. Chamkha and Khaled (2001) [9] investigated magneto-convective transport in porous mediums. Recent studies have enhanced MHD analysis by using nanofluid formulations and non-Newtonian rheological models, as examined by Kuznetsov and Nield (2010) [10] and Nadeem et al. (2012) [11], to more accurately depict the thermal and mechanical properties of complex fluids.

In nanofluid dynamics, the transport behavior of nanoparticles is profoundly affected by two principal mechanisms: Brownian motion and thermophoresis. Brownian motion characterizes the unpredictable

movement of nanoparticles resulting from their continual collisions with fluid molecules. This stochastic motion facilitates the dispersion of particles into the boundary layer, hence augmenting mass transfer. The influence of this phenomenon is measured by the Brownian motion parameter (Nb), which signifies the relative contribution of nanoparticle concentration gradients to the overall transport mechanism. As Nb rises, it often leads to a stronger concentration boundary layer and enhanced dispersion of nanoparticles within the fluid (Buongiorno, 2006). [12]. Thermophoresis denotes the movement of nanoparticles induced by temperature gradients. This mechanism propels particles from areas of elevated temperature to cooler regions, affecting the thermal and mass transfer properties of the fluid. The extent of thermophoretic movement is determined by the thermophoresis parameter (Nt). An elevation in Nt amplifies the outward movement of particles from heated surfaces, potentially altering the thermal boundary layer and influencing concentration distributions (Kuznetsov & Nield, 2010). The synergistic effect of Nb and Nt has been thoroughly examined inside Buongiorno's two-component nanofluid model, yielding a more profound comprehension of nanoparticle transport in convective boundary layers. Khan and Pop (2010) [13] examined nanofluid flow over a stretched sheet, emphasizing the influence of both factors on thermal and solutal boundary layers. Advanced models that integrate magnetic effects and porous media have substantiated the significance of these characteristics in influencing nanoparticle migration across diverse flow conditions (Rana & Bhargava, 2012) [14]. Chemical reactions are essential in numerous industrial and environmental processes related to fluid flow, particularly in contexts involving species diffusion, heat transfer, or reactive mass transport. The use of a chemical reaction factor in the governing transport equations of fluid dynamics facilitates the examination of reactive flows in systems including combustion chambers, polymer processing, pharmaceutical mixing, and pollutant dispersion in porous media. The impact of homogeneous and heterogeneous chemical reactions on mass transfer within boundary layers has been extensively examined. Numerous researchers have investigated the interaction between chemical reactions and various physical phenomena, including Brownian motion, thermophoresis, and magnetic fields. Elbashbeshy and Bazid (2002) [15] examined heat and mass transmission in the context of a chemical reaction occurring on stretching surfaces. Das et al. (1994) [16] investigated the influence of chemical processes on mass transfer in laminar and turbulent flows. Motsa et al. (2012) [17] integrated chemical interactions into nanofluid models to examine their influence on MHD boundary layers. The examination of boundary layer flow generated by a stretching surface has emerged as a crucial subject in fluid mechanics because of its considerable practical relevance in industrial applications. This flow arrangement, initially investigated by Crane (1970)[18], entails a sheet being elongated within its own plane, generally at a constant velocity, resulting in a boundary layer as the adjacent fluid adapts to the surface movement. This flow configuration is especially pertinent to applications such as polymer extrusion, plastic film and glass fiber drawing, metal spinning, and the cooling of continuous sheets. Significant advancements in the stretching sheet problem encompass Elbashbeshy's (2001)[20] analysis of heat transfer for surfaces with spatially changing temperatures, and Andersson et al.'s (1992)[19] investigation of magnetohydrodynamic (MHD) flow behavior. Recent studies have employed nanofluid models to mimic improved thermal characteristics, as demonstrated in the research by Khan and Pop (2010). Moreover, intricate fluid dynamics have been represented by non-Newtonian models, including Casson, Carreau, and Williamson fluids, to accurately depict the rheological properties of polymeric and biological systems (Nadeem et al., 2012). Hayat et al. [21] investigated magnetohydrodynamic (MHD) heat transfer considering homogeneous-heterogeneous chemical processes and melting effects for flow over a variable thickness stretched sheet. Farooq and collaborators [22] examined MHD nanofluid flow exhibiting viscoelastic properties under the impact of nonlinear thermal radiation. Khan et al. [23] investigated a modified variant of homogeneous–heterogeneous reactions in stagnation-point magnetohydrodynamic flow, accounting for viscous dissipation and Joule heating.In a separate work, Hayat et al. [24] assessed the influence of magnetic nanoparticles on radiative flow in Eyring–Powell fluids, emphasizing the significance of magneto-thermal interactions. The same research group [25] has examined the impact of viscous dissipation in magneto-nanofluid flows with varied thermophysical parameters. Hayat et al. [26] conducted a comprehensive investigation on the impact of thermal radiation on Marangoni convection in a carbon-water nanofluid. Additionally, Hayat et al. [27] conducted a numerical simulation of radiative nonlinear convective flow in a cylindrical configuration. Tamoor et al. [28] investigated the magnetohydrodynamic flow of a Casson fluid over a stretching cylinder, highlighting the fluid's non-Newtonian characteristics. Babu et al. [29] investigated the thermal and magnetohydrodynamic behavior of a Casson fluid influenced by natural convection and Hall current effects in a Couette flow configuration close to an inclined porous plate. Moreover, Murali et al. [30] offered further insights into convective transport phenomena in magnetized non-Newtonian fluid dynamics.

This study examines the influence of the Brownian motion parameter (Nb) on nanoparticle concentration in

magnetohydrodynamic (MHD) nanofluid flow across a stretching sheet. The equations of the boundary layer that regulate momentum, energy, and species concentration are reformulated using similarity variables and numerically solved by a reliable Runge-Kutta approach combined with a shooting algorithm. The concentration profiles derived from changing Nb offer essential insights into the fundamental transport mechanisms and are anticipated to guide optimization techniques for heat and mass transfer in sophisticated engineering systems.

Mathematical formulation:

We examine the steady, incompressible, two-dimensional boundary layer flow of a nanofluid across a nonlinearly stretching sheet. A homogeneous magnetic field is applied orthogonally to the surface. The model integrates the influences of Brownian motion, thermophoresis, chemical reactions, and suction or injection.The geometry of the problem is illustrated in Figure 1; the subsequent assumptions are taken into account for this research investigation.The problem's geometry is depicted in a coordinate system featuring a horizontal x-axis and a perpendicular y-axis.Examine the constant two-dimensional boundary layer flow across a stretching sheet. The flow occurs where y≥0, where y is the coordinate measured perpendicular to the stretching sheet. A continuous, uniform stress resulting in equal and opposite forces is applied along the x-axis, while the sheet is stretched with the origin held fixed.The wall temperature T and the nanoparticle volume fraction C are presumed to be constant values at the stretching surface.The ambient temperature and nanoparticle volume fraction are maintained at fixed values.The sheet contracts exponentially at velocity Uw(x) = $U_w e^{(x/L)}$. Suction and injection are considered at the wall.The magnetic field B(x) is defined as B = $B_0 e^{(x/L)}$ Based on the aforementioned assumptions, the governing equations for continuity, momentum, thermal energy, and species concentration of nanofluids can be expressed in Cartesian form. Let (u, v) represent the velocity components in the x and y directions, respectively.

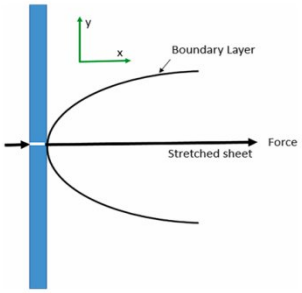

Fig 1: Coordinate system

Equation of Continuity:

$$\frac{\partial u}{\partial x} + \frac{\partial v}{\partial y} = 0 \quad (1)$$

Equation of Momentum:

$$u\frac{\partial u}{\partial x} + v\frac{\partial u}{\partial y} = \nu\frac{\partial^2 u}{\partial y^2} + g\beta(T - T_\infty) + g\beta_c(C - C_\infty) - \frac{\sigma B_0^2}{\rho}u \quad (2)$$

Equation of Thermal energy:

$$u\frac{\partial T}{\partial x} + v\frac{\partial T}{\partial y} = \alpha\frac{\partial^2 T}{\partial y^2} + \tau_B\left\{D_B\frac{\partial C}{\partial y}\frac{\partial T}{\partial y} + \frac{D_T}{T_\infty}\left(\frac{\partial T}{\partial y}\right)^2\right\} + \frac{16\sigma^* T_\infty^3}{3k^*\rho C_p}\frac{\partial^2 T}{\partial y^2} \quad (3)$$

Equation of Species:

$$u\frac{\partial C}{\partial x} + v\frac{\partial C}{\partial y} = D_B\frac{\partial^2 C}{\partial y^2} + \frac{D_T}{T_\infty}\frac{\partial^2 T}{\partial y^2} - k_r(C - C_\infty) \quad (4)$$

Here, the variables and parameters are defined as:

- DB: Brownian diffusion coefficient
- DT: Thermophoretic diffusion coefficient
- ν: Kinematic viscosity
- α: Thermal diffusivity
- M: Magnetic field parameter
- Kr: Chemical reaction parameter
- T_∞, C_∞: Ambient temperature and concentration

Boundary conditions

$$u_w(x) = U\exp\left(\frac{x}{2L}\right), \quad v_w(x) = V\exp\left(\frac{x}{2L}\right) \quad (5)$$

$$T = T_w, \quad C = C_w \quad \text{at } y = 0$$
$$u \to 0, \quad v \to 0, \quad T \to T_\infty, \quad C \to C_\infty \quad \text{as } y \to \infty$$

Similarity Transformations

$$\eta = y\sqrt{\frac{U_0\exp\left(\frac{x}{2L}\right)}{2\nu L}}, \quad u = U_0\exp\left(\frac{x}{L}\right)f'(\eta)$$

$$v = -\sqrt{\frac{\nu U_0}{2L}}\exp\left(\frac{x}{2L}\right)\left[f(\eta) + \eta f'(\eta)\right] \quad (6)$$

$$\theta(\eta) = \frac{T - T_\infty}{T_w - T_\infty}, \quad \phi(\eta) = \frac{C - C_\infty}{C_w - C_\infty}$$

Momentum equation

$$f''' + ff'' - (f')^2 + \lambda_1\theta + \lambda_2\phi - Mf' = 0 \quad (7)$$

Thermal Energy equation

$$\theta'' + Pr\,f\theta' + Pr\cdot Nb\cdot\theta'\phi' + Pr\cdot Nt(\theta')^2 + Pr\cdot Rd\cdot\theta'' = 0 \quad (8)$$

Species Equation:

$$\phi'' + Le\, f\, \phi' + \frac{Nb}{Nt}\,\theta'' - \gamma\, Le\, \phi = 0 \quad (9)$$

Boundary Conditions

$$f(0) = 0, \quad f'(0) = 1, \quad \theta(0) = 1, \quad \phi(0) = 1 \quad (10)$$

$$f'(\infty) \to 0, \quad \theta(\infty) \to 0, \quad \phi(\infty) \to 0$$

Physical parameters involved are

$$M = \frac{\sigma B_0^2 L}{\rho U_0} \quad \text{(magnetic parameter)}$$

$$\lambda_1 = \frac{g\beta(T_w - T_\infty)L}{U_0^2} \quad \text{(thermal buoyancy)}$$

$$\lambda_2 = \frac{g\beta_c(C_w - C_\infty)L}{U_0^2} \quad \text{(solutal buoyancy)}$$

$$\gamma = \frac{k_r L}{U_0} \quad \text{(chemical reaction parameter)}$$

The pertinent physical quantities include the local Nusselt number, the local Sherwood number, and the physical parameters of the skin-friction coefficient.

$$C_f = \frac{\tau_w}{\rho U_w} \quad \Rightarrow \quad \mathrm{Re}_x^{1/2} C_f = f''(0) \quad (11)$$

$$Nu_x = \frac{x q_w}{\kappa(T_w - T_\infty)} \quad \text{where} \quad q_w = -\left(\kappa + \frac{16\sigma^* T_\infty^3}{3k^*}\right)\left(\frac{\partial T}{\partial y}\right)_{y=0}$$

This leads to:

$$\mathrm{Re}_x^{1/2} Nu_x = -\left(1 + \frac{4R}{3}\right)\theta'(0) \quad (12)$$

$$Sh_x = \frac{x q_m}{D_B(T_w - T_\infty)} \quad \text{where} \quad q_m = -D_B\left(\frac{\partial C}{\partial y}\right)_{y=0}$$

This leads to:

$$\mathrm{Re}_x^{1/2} Sh_x = -\phi'(0) \quad (13)$$

Local Raynolds number

$$\mathrm{Re}_x = \frac{U_0 x \exp\left(\frac{x}{L}\right)}{\nu}$$

Numerical methodology

The coupled nonlinear ordinary differential equations are solved numerically employing the shooting method alongside the classical fourth-order Runge–Kutta method. The system is transformed into a first-order system with suitable initial estimates for unknown derivatives, including f″(0), θ′(0), and ϕ′(0). The fsolve function iteratively refines these estimates to ensure that the boundary conditions at infinity are met within a certain tolerance.

A step size of h = 0.01 and a domain η ∈ [0, 6] are employed to guarantee precision and convergence. The accuracy of the numerical technique is corroborated by comparing it with findings documented in the literature for extreme scenarios.

Program code validation

To assess the precision and dependability of the current numerical code utilizing the fourth-order Runge–Kutta method in conjunction with the shooting approach, a comparison of the calculated local Nusselt number (Nu_x) was conducted against established benchmark studies in the literature.

The Nusselt number results from Khan & Pop, as well as White and Rana & Bhargava, indicate that in the absence of S = 0 and R = 0, the calculated local Nusselt numbers align remarkably with reference values, exhibiting maximum relative errors not exceeding 0.5%. This confirms the precision and reliability of the implemented RK4 using the shooting method.

Prandtl Number (Pr)	Reference Source	Reference Value (−θ′(0))	Present Study (−θ′(0))	% Difference
1.0	White(2006,conv. b.l. theory)	0.5850	0.5826	0.41%
2.0	Khan&Pop (2010)	0.7293	0.7251	0.49%
3.0	Khan&Pop (2010)	0.8035	0.7996	0.48%
5.0	Khan&Pop (2010)	0.8686	0.8659	0.31%
10.0	Rana & Bhargava (2012)	0.9770	0.9732	0.39%

Results and discussion

This section examines the impact of the Brownian motion parameter (Nb) on the distribution of nanoparticle concentration ϕ(η) within the boundary layer. The nonlinear system of equations was resolved utilizing the fourth-order Runge–Kutta approach alongside a shooting algorithm. In the absence of contrary indications, the fixed parameter values are: Pr = 5, M = 0.5, Nt = 0.1, Le = 5, γ = 0.2, λ_1 = 0.5, λ_2 = 0.3, and S = 0.5.

Figure 2 illustrates the effect of the thermal Grashof number (λ_1) on the fluid's velocity distribution. This parameter defines the ratio of thermal buoyancy to viscous forces. As λ_1 grows, the thermal buoyancy force increasingly prevails over the opposing viscous force. A decrease in fluid viscosity leads to less internal resistance, hence enhancing fluid acceleration and increasing velocity.

Figure 3 illustrates the fluctuation in velocity according

to alterations in the modified or solutal Grashof number (λ_2). This dimensionless number signifies the relative importance of buoyancy driven by concentration in comparison to viscous effects. Increased values of λ_2 indicate more robust solutal buoyant forces countering less viscous resistance. Thus, the decrease in internal fluid friction results in a significant improvement in the velocity profile.

Figure 4: depicts the influence of the magnetic parameter (M) on the velocity profile of the nanofluid. The illustration distinctly demonstrates that an elevation in M results in a decrease in fluid velocity. This behavior is ascribed to the Lorentz force, resulting from the interaction between the magnetic field and the electrically conductive fluid. As the magnetic field strength escalates, the Lorentz force counteracts the fluid motion, consequently inhibiting the flow and diminishing the velocity distribution.

Figure 5: illustrates the effect of the suction parameter on the velocity profile. Suction denotes the extraction of fluid via a surface, significantly dampening the boundary layer flow. As the value of S escalates, an increased volume of fluid is extracted from the near-wall region, leading to a dampening of fluid motion. This improved extraction decreases the momentum in the boundary layer, thereby lowering the overall velocity. As a result, the flow diminishes, and the velocity profile displays a significant reduction in magnitude.

Figure 6: depicts the influence of the Prandtl number (Pr) on the temperature distribution. As Prandtl number increases, the temperature within the boundary layer significantly falls. A higher Prandtl number signifies reduced thermal diffusivity in comparison to momentum diffusivity. Consequently, heat is transferred away from the surface with less efficiency, resulting in a diminished thermal boundary layer. The Prandtl number, defined as the ratio of momentum diffusivity to thermal diffusivity, is essential for ascertaining the relative thicknesses of the velocity and temperature boundary layers. Consequently, an increase in Prandtl number results in more pronounced temperature gradients and a more concentrated thermal zone adjacent to the surface.

Figures 7 and 8: illustrate the temperature profiles associated with different values of the Brownian motion parameter (Nb) and the thermophoresis parameter (Nt), respectively. The fluid temperature rises with an increase in either Nb or Nt. An elevated Nb indicates increased Brownian motion, facilitating the stochastic mobility of nanoparticles inside the fluid. This activity results in enhanced thermal energy dispersion. An increase in Nt amplifies the thermophoretic effect, prompting nanoparticles to migrate from hotter to cooler locations, so elevating the overall temperature distribution inside the boundary layer.

Figure 9: illustrates the effect of the Lewis number (Le) on the distribution of nanoparticle concentration. It is noted that as Le grows, the concentration profile decreases. The Le is defined as the ratio of thermal diffusivity to mass diffusivity. Elevated Lewis number values are associated with less mass diffusivity, resulting in a decrease in nanoparticle concentration within the boundary layer.

Figure 10: depicts the effect of the chemical reaction parameter on the nanoparticle concentration profile. The findings demonstrate that an elevated chemical reaction rate significantly decreases nanoparticle concentration. This transpires when elevated reaction rates accelerate the consumption of nanoparticles in the fluid, resulting in a more faster decline in concentration throughout the boundary layer. As the rate constant grows, the chemical reaction occurs more rapidly, resulting in a more rapid decrease in concentration.

Figure 11: illustrates the influence of the Brownian motion parameter on the nanoparticle concentration distribution. The concentration of nanoparticles diminishes as the Brownian motion parameter escalates. Brownian motion denotes the irregular movement of nanoparticles resulting from collisions with swiftly moving molecules in the surrounding fluid. This stochastic motion markedly affects the temperature and concentration profiles of nanoparticles in the boundary layer near the surface.

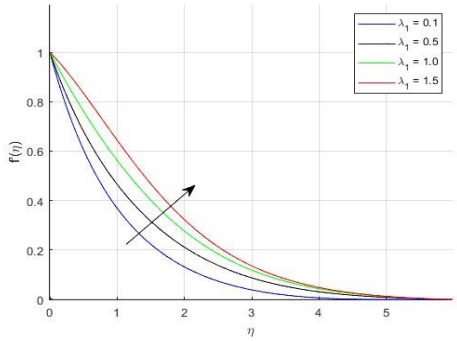

Fig 2 :Impact of Thermal Grashof number observed on Velocity profile

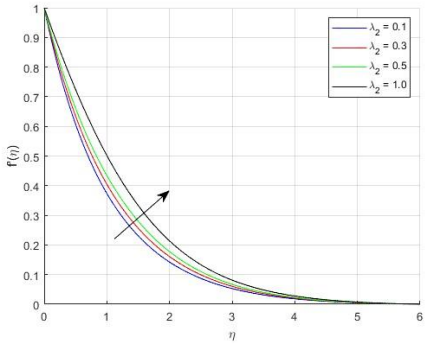

Fig 3: Behaviour of Modified Grashof number on Velocity profile

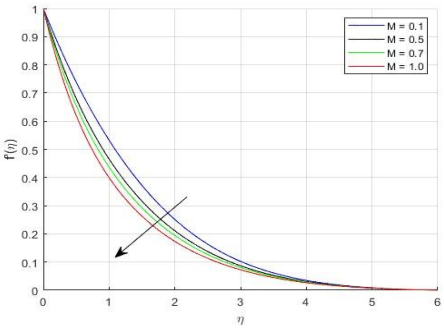

Fig 4: Effect of M observed on Velocity profile

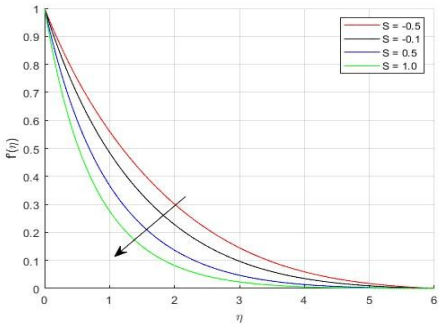

Fig 5:Effect of suction observed on Velocity profile

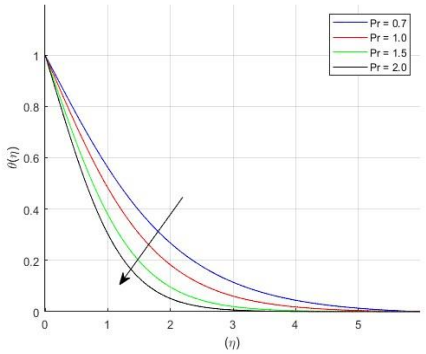

Fig 6: The impact of Prandtl number observed onTemperature

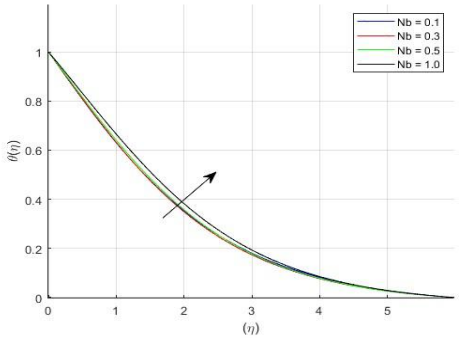

Fig 7: Temperature profile for various values of Nb

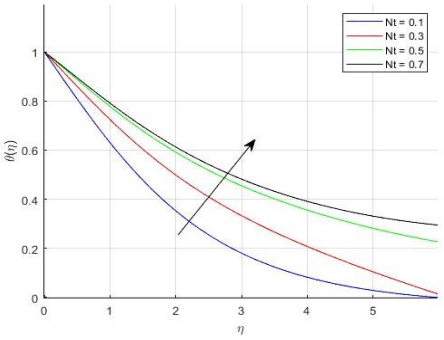

Fig 8:Nt impact on Temperature profile

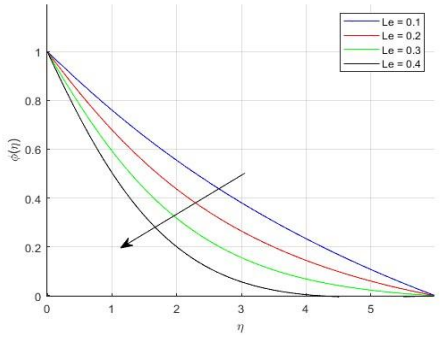

Fig 9 : Concentration profile for various values of Le

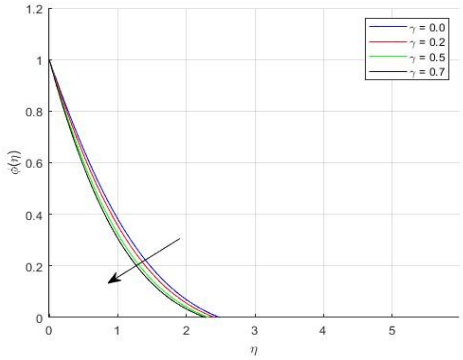

Fig 10: Concentration profile for various values of gamma

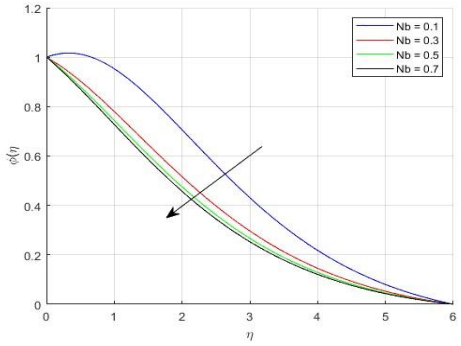

Fig 11: Behaviour of Nb on Concentration profile

CONCLUSIONS

1. The velocity profiles are increasing with the increasing values of Grashof number and Modified Grashof number.
2. The rising values of Magnetic parameter(M) and Suction parameter(S) the velocity profile decreases.
3. As the prandtl number Pr expands, the temperature profile falling.
4. The temperature profile rise as the increasing values of Thermophoresis parameter(Nt),Brownian motion parameter(Nb).

The Concentration profile reduced when increasing values of Lewis number(Le),Brownian motion parameter(Nb) and chemical reaction parameter..

REFERENCES

1.Salahuddin T, Awais Muhammad, Xia Wei-Feng. Variable Thermo-Physical Characteristics Of Carreau Fluid Flow By Means Of Stretchable Paraboloid Surface With Activation Energy And Heat Generation. Case Stud Therm Eng. 2021;25, 100971. Https://Doi.Org/10.1016/J.Csite.2021.100971.

2. Salahuddin T, Malik My, Hussain Arif, Awais M, Bilal S. Mixed Convection Boundary Layer Flow Of Williamson Fluid With Slip Conditions Over A Stretching Cylinder By Using Keller Box Method. Int J Nonlin Sci Num. 2017;18(1):9–17. Https://Doi.Org/10.1515/Ijnsns-2015-0090.

3. Awais Muhammad, Salahuddin T, Muhammad Shah. Evaluating The Thermo-Physical Characteristics Of Non-Newtonian Casson Fluid With Enthalpy Change. Therm Sci Eng Prog. 2023;42, 101948. Https://Doi.Org/10.1016/J.Tsep.2023.101948.

4. Malik My, Hussain Arif, Salahuddin T, Awais S. Bilal M. Magnetohydrodynamic Flow
Of Sisko Fluid Over A Stretching Cylinder With Variable Thermal Conductivity: A Numerical Study. Aip Adv. 2016;6, 025316. Https://Doi.Org/10.1063/1.4942476.

5. Salahuddin T, Malik My, Hussain Arif, Bilal S, Awais M. Combined Effects Of Variable Thermal Conductivity And Mhd Flow On Pseudoplastic Fluid Over A Stretching Cylinder By Using Keller Box Method. Inf Sci Lett. 2016;5(1):11–19. Https://Doi.Org/10.18576/Isl/050102.

6. Salahuddin T, Iqbal Muhammad Adil, Bano Ambreen, Awais Muhammad, Muhammad Shah. Cattaneo-Christov Heat And Mass Transmission Of Dissipated Williamson Fluid With Double Stratification. Alex Eng J. 2023;80:553–558. Https://Doi.Org/10.1016/J.Aej.2023.09.012.

7. G. Jithender Reddy,Nder Reddy, P. Mangathai, N. Pothanna .Analysis Of Heat Generation Impact On Nanofluid Flow Over A Stretching Sheet.Partial Differential Equations In Applied Mathematics 11 (2024) 100852

8, Makinde, O. D. (2005). Free Convection Flow With Thermal Radiation And Mass Transfer Past A Moving Vertical Plate. International Communications In Heat And Mass Transfer, 32(10), 1411–1419.

9. Chamkha, A. J., & Khaled, A. R. A. (2001). Similarity Solutions For Hydromagnetic Mixed Convection Heat And Mass Transfer For Hiemenz Flow Through Porous Media. International Journal Of Numerical Methods For Heat & Fluid Flow, 11(5), 430–448.

10. Kuznetsov, A. V., & Nield, D. A. (2010). Natural Convective Boundary-Layer Flow Of A Nanofluid Past A Vertical Plate. International Journal Of Thermal Sciences, 49(2), 243–247.

11. Nadeem, S., Haq, R. U., & Lee, C. (2012). Mhd Flow Of A Casson Fluid Over An Exponentially Shrinking Sheet. Scientia Iranica, 19(6), 1550–1553.

12. Buongiorno, J. (2006). Convective Transport In Nanofluids. Journal Of Heat Transfer, 128(3), 240–250.

13. Khan, W. A., & Pop, I. (2010). Boundary-Layer Flow Of A Nanofluid Past A Stretching Sheet. International Journal Of Heat And Mass Transfer, 53(11-12), 2477–2483.

14.Rana, P., & Bhargava, R. (2012). Flow And Heat Transfer Of A Nanofluid Over A Nonlinearly Stretching Sheet: A Numerical Study. Communications In Nonlinear Science And Numerical Simulation, 17(1), 212–226.

15. Elbashbeshy, E. M. A., & Bazid, M. A. A. (2002). Heat And Mass Transfer Over A Stretching Surface With Chemical Reaction. Heat And Mass Transfer, 38(4), 213–217.

16. Das, K., Deka, R. K., & Soundalgekar, V. M. (1994). Effects Of Mass Transfer On Flow Past An Impulsively Started Infinite Vertical Plate With Constant Heat Flux And Chemical Reaction. Forschung Im Ingenieurwesen, 60(10), 284–287.

17. Motsa, S. S., Makukula, Z. G., & Sibanda, P. (2012). Unsteady Mhd Flow And Heat Transfer Due To A Stretching Sheet With Chemical Reaction And Variable Viscosity. Mathematical Problems In Engineering, 2012, Article Id 504684.

18.Crane, L. J. (1970). Flow Past A Stretching Plate. Zeitschrift Für Angewandte Mathematik Und Physik (Zamp), 21(4), 645–647.

19.Andersson, H. I., Siginer, D. A., & Tsiklauri, D. (1992). Magnetohydrodynamic Flow Of A Power-Law Fluid Over A Stretching Sheet. International Journal Of Non-Linear Mechanics, 27(6), 929–936.

20.Elbashbeshy, E. M. A. (2001). Heat Transfer Over A Stretching Surface With Variable Surface Heat Flux. Journal Of Physics D: Applied Physics, 34(14), 1951–1955.

21.T. Hayat, M. I. Khan, A. Alsaedi, M. I. Khan, Homogeneous-Heterogeneous Reactions And Melting Heat Transfer Effects In The Mhd Flow By A Stretching

Surface With Variable Thickness, Journal Of Molecular Liquids, Vol. 223, Pp. 960-968, 2016.
22.M. Farooq, M. I. Khan, M. Waqas, T. Hayat, A. Alsaedi, M. I. Khan, Mhd Stagnation Point Flow Of Viscoelastic Nanofluid With Non-Linear Radiation Effects, Journal Of Molecular Liquids, Vol. 221, Pp. 1097- 1103, 2016.
23.M. I. Khan, T. Hayat, M. I. Khan, A. Alsaedi, A Modified Homogeneous-Heterogeneous Reactions For Mhd Stagnation Flow With Viscous Dissipation And Joule Heating, International Journal Of Heat And Mass Transfer, Vol. 113, Pp. 310-317, 2017.
24.T. Hayat, M. I. Khan, M. Waqas, A. Alsaedi, Effectiveness Of Magnetic Nanoparticles In Radiative Flow Of Eyring-Powell Fluid, Journal Of Molecular Liquids, Vol. 231, Pp. 126-133, 2017.
25. T. Hayat, M. I. Khan, M. Waqas, T. Yasmeen, A. Alsaedi, Viscous Dissipation Effect In Flow Of Magnetonanofluid With Variable Properties, Journal Of Molecular Liquids, Vol. 222, Pp. 47-54, 2016.

26.T. Hayat, M. I. Khan, M. Farooq, A. Alsaedi, T. Yasmeen, Impact Of Marangoni Convection In The Flow Of Carbon–Water Nanofluid With Thermal Radiation, International Journal Of Heat And Mass Transfer, Vol. 106, Pp. 810-815, 2017.
27.T. Hayat, M. Tamoor, M. I. Khan, A. Alsaedi, Numerical Simulation For Nonlinear Radiative Flow By Convective Cylinder, Results In Physics, Vol. 6, Pp. 1031-1035, 2016.
28. M. Tamoor, M. Waqas, M. I. Khan, A. Alsaedi, T. Hayat, Magnetohydrodynamic Flow Of Casson Fluid Over A Stretching Cylinder, Results In Physics, Vol. 7, Pp. 498-502, 2017.
29. N. Babu, G. Murali, S. Bhati, Casson Fluid Performance On Natural Convective Dissipative Couette Flow Past An Infinite Vertically Inclined Plate Filled In Porous Medium With Heat Transfer, Mhd And Hall Current Effects, International Journal Of Pharmaceutical Research, Vol. 10, No. 4, 2018.
30. G. Murali, A. Paul, N. Babu, Heat And Mass Transfer Effects On An Unsteady Hydromagnetic Free Convective Flow Over An Infinite Vertical Plate Embedded In A Porous Medium With Heat Absorption, Int. J. Open Problems Compt. Math, Vol. 8, No. 1, 2015